# Lensed fibre-array assembly with individual fibre fine positioning in the sub-micron range

# Lensed Fiber-Array Assembly With Individual Fiber Fine Positioning in the Submicrometer Range

Johan H. C. van Zantvoort, Simon G. L. Plukker, Erwin C. A. Dekkers, Georgi D. Petkov, G. D. Khoe, *Fellow, IEEE*, Antonius M. J. Koonen, *Senior Member, IEEE*, and Huug de Waardt, *Associate Member, IEEE*

***Abstract*—An innovative design is presented enabling fine positioning of each individual fiber in a fiber array used in multiinput- and multioutput-port photonic integrated circuits. Hence, the coupling efficiency of lensed fiber arrays can be improved by eliminating the eccentricities of the lenses deposited on the individual fibers and the inaccuracies of the supporting V-groove substrates. In preparation, four different types of commercially available lensed fibers are characterized and coupling efficiencies to InP-based waveguides are determined in order to select the best applicable fibers for the array. The final fiber-tip position accuracy is within $\pm 0.25$ $\mu$m and this design is based on metal deformation by laser-welding-induced local heat. With this technique, laser-supported adjustment is possible, allowing the opportunity of fine-tuning the fiber-tip position of already secured parts in the subassembly. Owing to the accurate fiber-tip position and the assembly of the array with selected lensed fibers, coupling efficiencies of $-2.9$ to $-3.5$ dB are simultaneously measured for four fibers to InP-based waveguides with physical dimensions of 3 $\mu$m $\times 0.6$ $\mu$m. To compare these results, the performance of different types of regular, commercially available fiber arrays, whereby the fibers are mounted on silicon V-groove substrates, are determined. In contrast, the measured coupling efficiencies are of the order of $-5.2$ to $-7.8$ dB using similar InP-based waveguides.**

***Index Terms*—Fiber chip coupling, laser adjustment, lensed fiber array, waveguide.**

## I. Introduction

EFFICIENT fiber-to-chip coupling is an essential requirement for high-performance optoelectronic devices. One of the available substrate materials for fabrication of optoelectronic devices is indium phosphide (InP), which is considered to be the ideal substrate material for the third-generation monolithically integrated photonic components [1].

Owing to the high refractive index, the planar bendings of the waveguides can be realized with radii of up to approximately 100 $\mu$m. Consequently, more functions per unit area can be implemented in comparison with glass- or polymer-based devices. Active and passive components can be integrated on one single InP-based chip; moreover, InP is suitable for the integration of electrical circuit functions.

In spite of all these advantages, the high refractive index contrast between the waveguides and the monomode fibers results in optical coupling losses of 10 dB. Therefore, mode-shape matching is necessary to reduce the optical losses in mode mismatch of the small elliptical widely divergent field of the waveguide (typical near-field waveguide dimensions are 3 $\mu$m $\times$ 0.6 $\mu$m) compared to the ten times larger circular field of a single-mode fiber with a narrow angle of acceptance.

As a result of advanced integration technologies, multiple optical components such as arrayed waveguide gratings for wavelength (de)multiplexing, modulators, switches and couplers (passive components) also laser diodes, photodetectors, and semiconductor optical amplifiers (active components) can be integrated into multifunctional devices, which require multiple fiber connections [2].

The bottleneck in this multiple fiber connection is the inaccuracy of fiber arrays, due to the core eccentricity of the individual fibers. In [3], fibers are partially metal coated so the core position can be aligned by rotating the fiber. In a previous paper, we characterized the eccentricities of individual fibers with measured eccentricities varying from 0.2 to 2 $\mu$m. Fibers with a similar core eccentricity can be selected and mounted in a V-groove by rotating the fibers according to the direction of the eccentricity [4]. To overcome the problem of core eccentricity, a design is developed to assemble fiber arrays whereby each individual fiber can be aligned independently.

This paper is organized as follows. Section II presents an overview of different types of commercially available lensed fibers, which have been characterized to select the best suitable fibers in combination with the used waveguides. Thereafter, the laser adjust mechanism is explained in Section III. Section IV sketches the design of the array assembly. Section V describes the assembly and fine-align processes of the fiber array. Section VI characterizes the assembled fiber array. Section VII compares the results with commercially available types of lensed fiber arrays. Section VIII provides conclusions and Section IX gives recommendations.

## II. Characterization of Commercially Available Lensed Fibers

Since the realization of the first diode lasers operating in the 1.3-$\mu$m-wavelength region for fiber-optics communication [5], different methods for efficient coupling of light in the fiber have been reported. A cost-effective method for aligning and fixing the fiber to an optical device, is to attach the lens directly to the fiber. Hence, the lens reduces coupling losses between an optical device and the fiber. With regard to fiber-tip fabrication, different technologies can be used; photolithographic technique [6]–[8], drawing technique using arc discharge of an arc welder fusion splicer [9]–[11], drawing technique and lens fabrication by using

Manuscript received August 23, 2005; revised May 12, 2006. This work was supported by the Netherlands Organization for Scientific Research under the "NRC photonics" Grant.

The authors are with Eindhoven University of Technology, 5600 MB Eindhoven, The Netherlands (e-mail: j.h.c.v.zantvoort@tue.nl; a.m.j.koonen@tue.nl).

Digital Object Identifier 10.1109/JSTQE.2006.882633

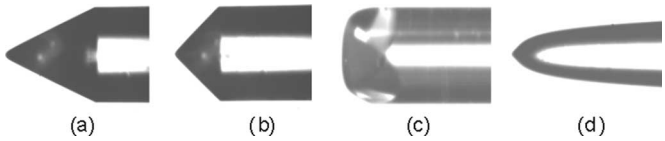


Fig. 1. Different types of fiber tips. Hemispherical (a) fiber type A and (b) fiber type B. Elliptically focused (c) fiber type C and (d) fiber type D.

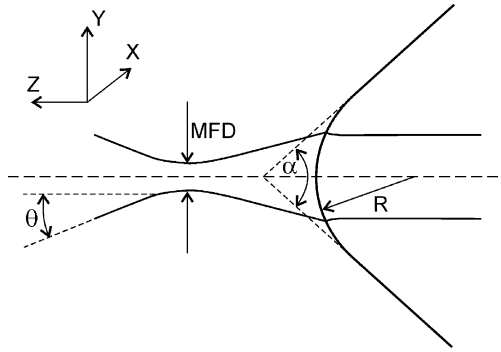


Fig. 2. Explanation of the parameters used in Table I. $R$ is the radius of the fiber tip; $\alpha$ is the tapered angle of the fiber tip; $D_x, D_y$, and $D_z$ are the alignment tolerances that produce an additional optical coupling loss increment of 1 dB in the $x$-, $y$-, and $z$-directions; $\theta$ is the far-field angular radius (half-angle divergence) of the Gaussian beam, defined for the numerical aperture $\mathrm{NA} = n \sin\theta$, determined at the 13.5% $(1/e^2)$ intensity level; and MFD is the mode-field diameter of the Gaussian beam.

high-index glass [12], electric arc discharge technique to fuse a small silica rod to a cleaved fiber, which forms a hemispherical lens after further arc heating [13], chemical etching [14], [15] or a combination of chemical etching and electric arc discharge technique [16], laser micromachining [17], mechanical grinding and polishing [18], and mechanical grinding and polishing in combination with the electric arc discharge technique [19].

After 25 years of research, only a few companies in the world manufacture lensed fiber tips with the techniques mentioned in Section II. Continuing this research, the specifications of the fiber tips are compared and the coupling efficiencies between monomode InP-based waveguides and lensed fibers are measured for hemispherical fibers with lens radii of 5-, 10-, and 15 $\mu$m. The lensed fiber tips with radii of 5 and 10 $\mu$m are manufactured with two different wedge-tapered angles $\alpha$ of $50\,^\circ$ and $90\,^\circ$ (Fig. 1 (types A and B) and Fig. 2). Initially, the coupling efficiency is determined. Next, the displacements for a 1-dB coupling loss increment for the three linear displacements of the fiber in front of the waveguide are measured. Subsequently, a complete hemispherical far-field profile is measured using a three-dimensional (3-D)-scanning goniometric radiometer. From the far-field data, the numerical aperture is determined at the 13.5% $(1/e^2)$ intensity level and the mode field diameter is calculated. The results are summarized in Table I. From left to right are shown: $R$, the radius of the fiber tip in micrometers; $\alpha$, tapered angle of the fiber tip; $\eta$, the coupling efficiency between the fiber and the waveguide; $D_x, D_y, D_z$, the alignment tolerances resulting in an additional coupling loss of 1 dB in the lateral $x$-direction, transversal $y$-direction, and longitudinal $z$-direction; NA, the measured numerical aperture of the fiber; and MDF, the calculated mode field diameter of

TABLE I
MEASURED RESULTS OF HEMISPHERICAL LENSED FIBERS WITH RADII OF 15, 10, AND 5 $\mu$m

| R [μm] | α [°] | η [dB] | Dx [μm] | Dy [μm] | Dz [μm] | NA [-] | MDF [μm] |
|---|---|---|---|---|---|---|---|
| 15 | 50 | - 4.4 | ± 0.8 | ± 0.7 | ± 4 | 0.24 | 3.6 |
| 10 | 50 | - 3.6 | ± 0.7 | ± 0.6 | ± 3 | 0.26 | 2.9 |
| 10 | 90 | - 3.6 | ± 0.7 | ± 0.6 | ± 3 | 0.32 | 2.8 |
| 5 | 50 | - 4.1 | ± 0.6 | ± 0.4 | ± 2 | 0.48 | 2.1 |
| 5 | 90 | - 2.8 | ± 0.6 | ± 0.4 | ± 2 | 0.57 | 2 |

the Gaussian beam. The meaning of the used parameters is schematically sketched in Fig. 2. In conclusion, if the lens radius decreases, the numerical aperture increases whereas the mode field diameter decreases. Consequently, the coupling efficiency increases as a result of improved mode matching to the small, elliptical near-field and the widely diverging far-field of the waveguide. However, if the radii decrease, the Fresnel loss increases rapidly due to light that misses the lens or is internally reflected [9]. Therefore, the fiber tips are antireflection coated at 1550 nm, which reduces this phenomenon. The backreflections are measured and fibers with lens radii of 5 $\mu$m, in combination with wedge-tapered angles of $50\,^\circ$, show more reflections than the same wedge-shaped fibers with lens radii of 10 and 15 $\mu$m. This explains the relative high coupling loss of 4.1 dB. In contrast, fiber tips with radii of 5 $\mu$m and wedge-tapered angles of $90\,^\circ$ show the minimum backreflection and the best coupling efficiency of $-2.8$ dB. In addition, the numerical apertures of fibers with wedge-tapered angles of $90\,^\circ$ are also higher than fiber tips with tapered angles of $50\,^\circ$.

To complete the possibilities of fiber waveguide coupling efficiency improvement, elliptically imaged spot-sized fibers can be used [17], [19]–[24]. Two different elliptically imaged spot-sized fiber tips are investigated and both fiber tips are also shown in Fig. 1. The first fiber type C is chisel shaped and the radii of the lenses on the chisel tips vary between 5–12, 15, and 20 $\mu$m. Likewise, these fibers are antireflection coated at 1550 nm. The measured coupling efficiency for fibers with lens radii smaller than 10 $\mu$m is almost constant and limited to $-6.8$ dB for the optimum rotation angle of the fiber compared with the waveguide. When the lens radius is larger than 10 $\mu$m, the coupling losses only increase. The far-field profile of the fiber tips is measured and the radiation profile is elliptical if the lens radii are smaller than 12 $\mu$m and circular when the lens radii are larger than 15 $\mu$m. The second fiber type D has two different radii perpendicular to each other (Fig. 1) and also antireflection coated at 1550 nm. According to the data of the manufacturer, the two radii focused the infrared (IR) light to an elliptical spot of 1.7 $\mu$m $\times 3.6$ $\mu$m. For the optimum rotation angle, the measured efficiency is –4.1 dB. When the fiber is rotated $90\,^\circ$, the losses are 5.1 dB. These relatively high losses are caused by a prominent diffraction structure observed in the far-field profile.

In conclusion, both types of elliptical lensed fiber tips are not applicable for the array assembly in combination with monomode InP-based waveguides. The highest efficiency of

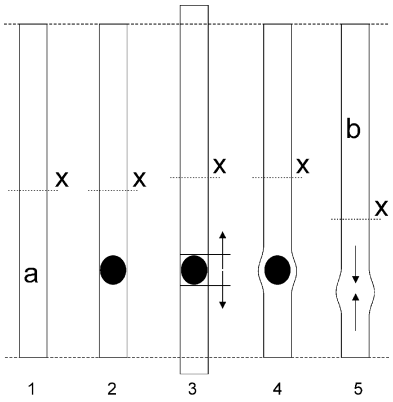


Fig. 3. Schematic presentation of laser-support-adjust mechanism. This mechanism is based on elastic and plastic material deformations. If a section [no. 1, position (a)] of a thin sheet of material is heated up locally (no. 2), the heated material expands elastically (no. 3). When the temperature of the material is further increased, the material deforms plastically if the expansion is obstructed (no. 4). After the heated part of the material is cooled down to room temperature, the shrinkage arises from the plastic deformation of the heated part (no. 5).

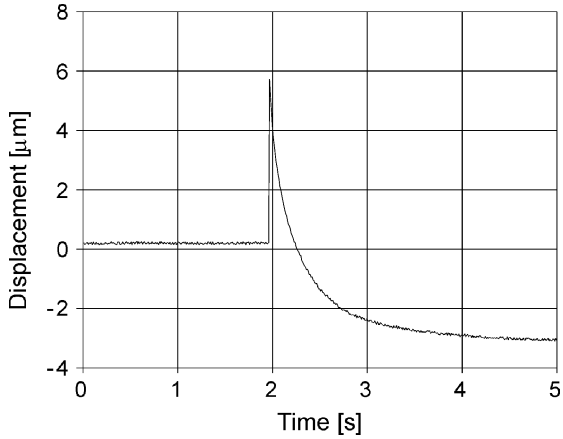


Fig. 4. Dynamic response from the middle position (x) of a metal sheet, which is sketched in Fig. 3, by heating up the metal sheet at position (a) locally (Fig. 3).

–2.8 dB is possible with fiber tips that are ground at wedge-tapered angles of $90^\circ$ in combination with lens radii of 5 $\mu$m.

## III. Laser Adjust Technology

Laser welding is acknowledged at present as the most stable technology for the fixation of fibers and lenses in optoelectronic devices [25], [26]. During the welding process, the solidification shrinkage of the welded parts causes misalignment of the components [27], [28]. Laser beam balance and symmetry are used to minimize these postweld shifts [29]. The laser hammering process that compensates for the postweld shifts is proven to be an effective application for single-fiber components. For multichannel devices, laser hammering is effectively applied in [30].

In the design presented in this paper, laser contraction technology is used. With this technique, laser-supported adjustment is possible with the opportunity of fine-tuning the position of already secured parts. This application is demonstrated for coupling fiber arrays to photonic chips in a previous paper [31]. As demonstrated in this reference, the coupling loss for four fiber-waveguide transitions is 5.7 dB/fiber-waveguide. This loss includes 4.4 dB due to the mode mismatch of the fiber tip with a lens radius of 15 $\mu$m and 1.3 dB due to the imperfection of the fiber array. The measured core positions vary in the range of 1–2 $\mu$m. Therefore, if the accuracy of the core positions and the coupling efficiency can be improved by using lensed fiber tips with smaller lens radii, the total coupling efficiency can be improved.

As mentioned in the previous paragraph, the applied mechanism for the fine positioning of the fiber tips individually is laser contraction, which is based on elastic and plastic material deformation. This mechanism is schematically shown in Fig. 3. If a sheet of material, (Fig. 3, no. 1) is heated up locally at position (a) by a Nd:YAG laser welder (Fig. 3, no. 2), the heated zone expands elastically (Fig. 3, no. 3). When this expansion is obstructed and the temperature of the material is further increased, the material deforms plastically (Fig. 3, no. 4). After the heated part of the material has cooled down to room temperature, the shrinkage arises from the plastic deformation of the heated part (Fig. 3, no. 5). Hence, this mechanism can be used as an actuator. Fig. 4 shows the dynamic response of heating up the metal sheet locally with a weld time of 5 ms and energy of 2.8 J. The experiment is similar to the metal sheet in Fig. 3. The position of the middle part (indicated by $x$ in Fig. 3) of the actuator sheet has been measured. The dimensions of the metal sheet are 30 mm $\times$ 1 mm $\times$ 0.2 mm, showing the length, width, and height, respectively. Both ends of the metal sheet are fixed. At the lower part of the metal sheet [Fig. 3, position (a)], the material is heated up locally. Initially, expansion is measured by the position sensor. After 3 s, the measured position of the metal sheet is shifted 3 $\mu$m in the direction of the heated zone of the metal sheet. During this process, internal stress in the metal sheet will be generated because of the plastic deformations. This stress is used for the fine-aligning process (in the range of 0.1–0.5 $\mu$m, approximately) that involves heating up the metal sheet with an enlarged area by defocusing the focusing head of the Nd:YAG laser welder at position (b) (Fig. 3, no. 5). Consequently, by heating up the metal sheet over a relatively large area, the internal stress and the elastic expansion of the heated area at position (b) result in a very small alignment step of the middle position ($x$) in the direction of position (a) (Fig. 3, no. 1). If the focusing head of the Nd:YAG laser welder is adjusted back in focus to deform the metal sheet plastically and shifted to an unheated position at the upper part (b) of the metal sheet, the middle part can be re-adjusted back in the opposite direction to position (b). The energy level whereby the metal sheet deforms plastically is 1.5 J, approximately. Below 1.5 J, the material is only heated up. The fine-adjust process of the middle position is achieved by gradually increasing the energies of the heated area at the same position from 0.8 to 1.7 J. Note that the heating up of the metal sheet is achieved by enlarging the heated area by defocusing the focusing head. This way, the energy density decreases, which locally results in a lower temperature profile.

The material used is invar, to benefit from the low coefficient of thermal expansion (CTE) and therefore suitable for optoelectronic packaging [32]. The minimum CTE of the used invar alloy, which contains 64% Fe and 36% Ni, at room temperature

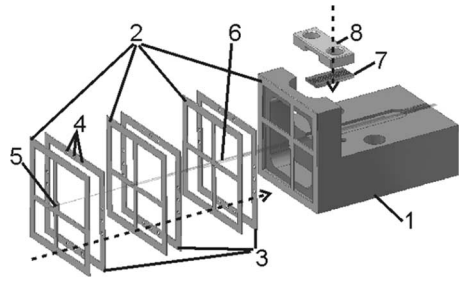


Fig. 5. Design to align fibers individually in a fiber array. The four fibers (6) are mounted in a V-groove substrate (7) and the four lensed fiber ends are mounted in four separated "cross shaped" adjust frames (2), thereby enabling individual positioning of the fiber tips. By heating the branches of the frames locally, the fiber tips can be aligned in the desired direction by using laser contraction technology.

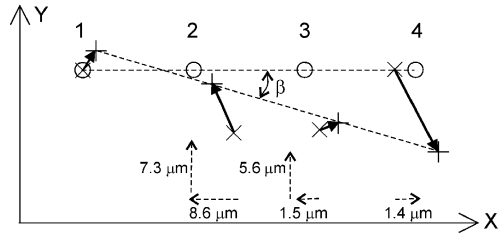


Fig. 6. Fiber numbering and definitions of the $x$- and $y$-axes used in this paper. The *marks* (x) are the fiber-core positions of the preassembled array in the initial state. The *marks* (o) are the preferred positions. The *dotted line arrows* show the executed translations that have to be made to achieve the preferred positions (o) of the fiber array. However, the final fiber-core positions of the assembled array are indicated with the $(+)$ *marks* as a result of crosstalk in the alignment frames. The *solid arrows* visualize the executed relative movement of the fiber tips. Consequently, the final fiber-core positions are slightly tilted at an angle $\beta$ of $0.03\,^{\circ}$ compared with the preferred positions (o).

is $1.3 \times 10^{-6}\,\mathrm{K}^{-1}$ [33]. The CTE is temperature dependent and increases at higher temperatures. At high temperatures, its magnitude is almost equal to ordinary metals and alloys [34]. Therefore, this material is also ideal and can be used as an actuator for the tuning frames. These frames are used for the assembly and are described in Section IV.

## IV. Fiber-Array Assembly Design

The fiber-array assembly is sketched in Fig. 5. The assembly consists of an L-shaped profile (1), four "cross-shaped" adjust frames (2), and three spacer plates (3). These spacer plates are fitted with three drilled holes with a diameter of 0.8 mm on each side (4), which are filled with gold brazing solder. The solder has a melting point of $950\,^{\circ}$C approximately. Initially, the four adjust frames and three spacer plates, filled with gold brazing solder are aligned and laser welded to the L-shaped profile. To reduce the internal stresses in the adjust frames, the subassembly is annealed at $1000\,^{\circ}$C, and at the same time, the gold brazing solder flows between the alignment frames and spacer plates to achieve a homogeneous fixation. Next, a hole (5) with a diameter of 280 $\mu$m is precisely drilled in the middle part of each adjust frame, through which the fibers (6) will be guided. Subsequently, a silicon V-groove substrate (7) is fixed to the L-shaped profile. The fibers are then guided through the holes of the adjust frames and put into the V-grooves, temporarily clamped between the V-groove substrate and a clamping bracket (8). After aligning the fiber tips in the longitudinal direction, the fibers are fixed to the adjust frames and the silicon V-groove substrate with epoxy. The width and thickness of the frames are 1 mm and 0.2 mm, respectively, and the total dimensions of the assembly are 30 mm $\times$ 20 mm $\times$ 20 mm, representing the length, width, and height, respectively.

The core positions of the fibers are measured actively by launching laser light into the fibers. A reference fiber opposite to the launched fiber is connected to an $x$-$y$-$z$ translation stage and receives the emitted light. Consequently, the maximum value of optical received power is a direct measure of the fiber core position in the three directions.

The translation stages in the lateral $x$- and longitudinal $z$-directions are the temperature-stabilized high-precision stages. The absolute position is measured by optical linear scales made of zerodure. The transversal $y$-direction is measured with a piezoelectric translation stage with active feedback, resulting in a final core position determination in three degrees of freedom (DOFs), with an accuracy of 0.05 $\mu$m. Further methods for measuring the $x$-$y$ core centers of fiber arrays by using direct comparison of the fiber core center position to a lithographically patterned template are published in [35]. Alternatively, fiber arrays can be compared with a standard reference array to reduce the measuring time [36].

Depending on the measured actual IR-spot position of the individual fibers in the preassembled fiber array, the fiber tips can be aligned based on the previously described process in Section III. This can be achieved by laser heating the positions concerned in the tuning frames. This process is described in detail in Section V.

## V. Fine-Alignment Procedure of the Fiber Array

After the subassembly is annealed and soldered in the same heat-treatment process, the four fiber holes are drilled precisely with regard to the silicon V-grooves and spaced at 500-$\mu$m intervals. Thereafter, the fibers are guided through the holes concerned in the adjust frames and aligned in the longitudinal $z$-direction using a fiber gripper mounted on a differential micrometer. The measured accuracy of adjustment in the $z$-direction is 0.1 $\mu$m approximately using a microscope with a high magnification factor. The fibers are fixed to the adjust frames by using a two-component room-temperature curing and low-viscosity adhesive, specially designed for glass bonding and suitable for the bonding of metals. With this procedure, it is also possible to assemble fiber arrays wherein the fiber tips protrude toward each other with an angle. These arrays can be used to adapt devices with tilted waveguides relative to the chip facet for reducing backreflection [37]. The layer thickness of adhesive between the fibers (diameter of 125 $\mu$m) and the holes (diameter of 280 $\mu$m) is symmetrically round and approximately 80-$\mu$m thick. According to the specifications of the adhesive, a layer of adhesive 50–100-$\mu$m thick will normally impart the greatest lap shear strength to a joint.

The fiber numbering and coordinate system used in this paper are illustrated in Fig. 6. The four focused fiber-spot positions

TABLE II
MEASURED CORE POSITIONS OF THE FOUR FIBERS OF THE PREASSEMBLED FIBER ARRAY AND THE FINAL CORE POSITIONS OF THE LASER-ADJUSTED FIBER ARRAY

| | Fiber core positions pre-assembled array | | Fiber core positions laser adjusted array | |
|---|---|---|---|---|
| Fiber | ΔX [μm] | ΔY [μm] | ΔX [μm] | ΔY [μm] |
| 1 | 0.0 | 0.0 | + 0.25 | + 0.25 |
| 2 | + 8.6 | - 7.3 | + 0.25 | - 0.25 |
| 3 | + 1.5 | - 5.6 | - 0.25 | + 0.2 |
| 4 | - 1.4 | 0.0 | + 0.05 | + 0.25 |

of the preassembled array have been measured actively and the results are shown in Table II. Taking fiber 1 as a reference, fiber 2 must align 8.6 $\mu$m in the negative $x$-direction and 7.3 $\mu$m in the positive $y$-direction (this movement, which has to be made to achieve the ideal fiber-tip position is also illustrated with the dotted line arrows in Fig. 6). Likewise, fiber 3 has to align 5.6 $\mu$m in the positive $y$-direction and 1.5 $\mu$m in the negative $x$-direction. Finally, fiber 4 has to be aligned 1.4 $\mu$m in the positive $x$-direction. The ideal fiber-tip positions are indicated by the circles (o) and the measured initial fiber-tip positions are shown by the four (x) marks in Fig. 6.

First, fiber 2 is laser adjusted over a range of 4.7 $\mu$m in the positive $y$-direction. We intended to translate fiber 3 in the positive $y$-direction too, but the first laser shot at the alignment frame of fiber 3 is probably executed with too low an energy to realize plastic deformation. As the fiber tip moved 1.4 $\mu$m in the opposite direction, hence only some expansion in the adjust frame occurred. After increasing the energy, fiber 3 is laser adjusted in the positive $y$-direction. However, the fiber also moved in the positive $x$-direction due to crosstalk in the alignment frame [Fig. 7(c)]. Therefore, fiber 4 is laser adjusted in the negative $y$-direction to compensate for the deviation of fibers 2 and 3 in the $y$-direction. The next sequence of adjusting the fibers is again fiber 2 in the negative $x$-direction. After this adjustment, all the fibers are within an accuracy of $\pm 1$ $\mu$m in the $y$-direction. Now fibers 2 and 3 have to be aligned 3.2 $\mu$m and 1.1 $\mu$m in the negative $x$-direction, respectively, but instead of adjusting these two fibers, fiber 1 is adjusted in the positive $x$-direction. Hence, due to crosstalk of the adjust frame again, fiber 1 is translated in the positive $y$-direction [Fig. 7(a)]. Consequently, fiber 1 is laser adjusted back in the negative $y$-direction and positive $x$-direction by heating up the opposite arms of the tuning frames. This indicates a large amount of internal stress in the adjust frames. This principle was used to adjust the four fibers in the next order: 1, 3, 2, 1, 3, 2, 4, 1, 3, 1, and finally fiber 2.

The measured fiber-spot positions subsequent to the laser-adjust process are also listed in Table II. The accuracy of the fiber-core positions is within $\pm 0.25$ $\mu$m and the absolute displacements of the fiber tips are shown in Fig. 7. Compared with the preferred fiber-tip positions [marked with (o)], the final positions [marked with (+)] are slightly tilted at an angle $\beta$ of $0.03^\circ$ (Fig. 6) as described in Section V. During the laser-adjusting process, crosstalk in the adjust frames of fibers 3 and 1 are measured. This can be improved by increasing the width of the adjust frames. A photograph of the realized array is shown in Fig. 8.

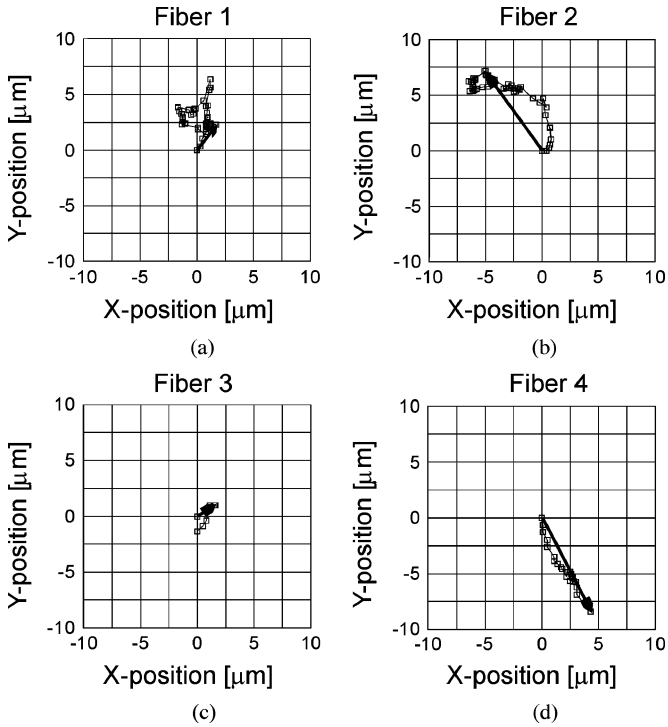


Fig. 7. Absolute movements of the four fiber tips during the laser-adjust fine-positioning process.

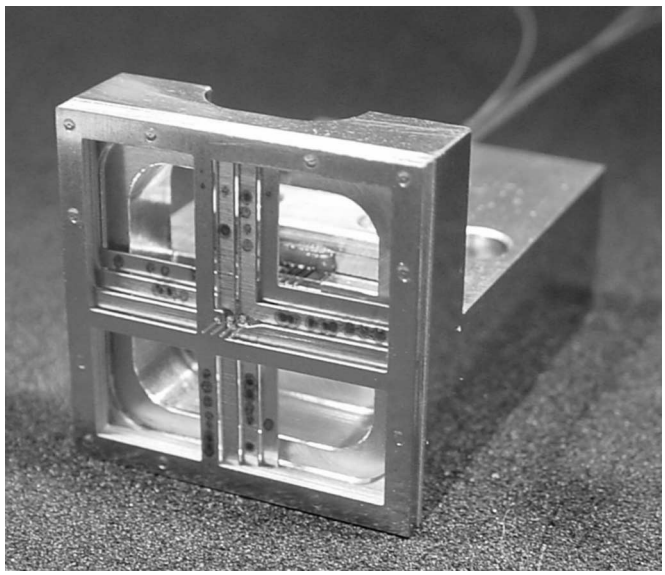

Fig. 8. Photograph of the realized fiber array. The fiber-core positions are laser adjusted within an accuracy of $\pm$ 0.25 $\mu$m.

## VI. CHARACTERIZATION OF THE ASSEMBLED FIBER ARRAY

The fiber array is mounted on a six-axis piezoelectric-controlled manipulator and positioned in front of an InP-based

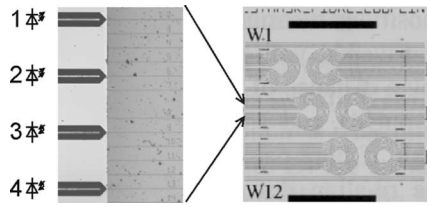


Fig. 9. Enlarged photograph of the assembled fiber array aligned to an InP-based optical chip (photograph *left*). Fibers 1 and 2 are connected to a laser source. Fibers 3 and 4 are connected to optical power meters. The light is transmitted from fibers 1 and 2 through the chip with optical looped waveguides (photograph *right*) and the light is received by fibers 3 and 4.

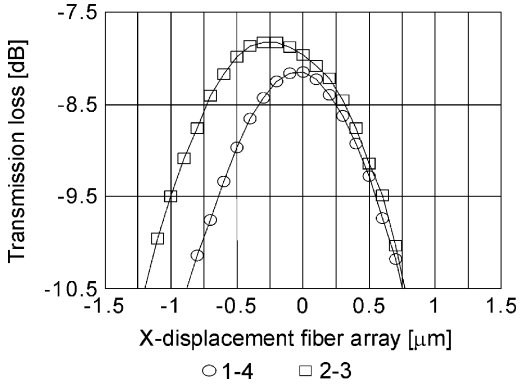


Fig. 10. Transmission curves of both fiber pairs combination 1–4 and 2–3 as a function of lateral displacement shift.

optical chip with looped waveguides (Fig. 9). The waveguides are 3 $\mu$m $\times 0.6\,\mu$m in lateral $x$- and transversal $y$-directions, respectively, and the chip facet is antireflection coated at 1550 nm. Fibers 1 and 2 are connected to a laser source, while fibers 3 and 4 are connected to optical power meters. The laser light emitted by fiber 1 is launched into the waveguide and guided through the chip to fiber 4. Similarly, laser light transmitted by fiber 2 is also guided by another looped waveguide to fiber 3. Fiber combination 1–4 is optimally aligned in all 6 DOFs and the fiber array is shifted over a range of 2 $\mu$m in the lateral $x$- and transversal $y$-directions. The transmission-loss curves for displacement in the $x$- and $y$-directions are shown in Figs. 10 and 11, respectively. The measured difference in both peak levels is 0.2 $\mu$m in both $x$- and $y$-directions. The total measured losses are 7.8 dB for fiber pair 1–4 and 8.2 dB for fiber pair 2–3. The estimated losses in the waveguides are in the order of 1.5–2 dB. Therefore, the coupling efficiency of the individual fiber is in the order of $-2.9$ to $-3.5$ dB. To compare the assembled fiber array with regular fabricated fiber arrays, the performance of commercially available lensed fiber arrays is described in Section VII.

## VII. Characterization of Commercially Available Fiber Arrays

Two different types of commercially available fiber arrays are characterized. Type E is assembled with drawn tapered fiber tips [Fig. 12(a)] while type F is assembled with ground and polished hemispherical fiber ends [Fig. 12(b)]. From both types, arrays

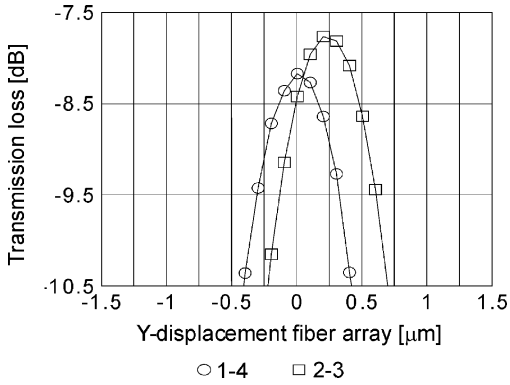


Fig. 11. Transmission curves of both fiber pairs combination 1–4 and 2–3 as a function of transversal displacement shift.

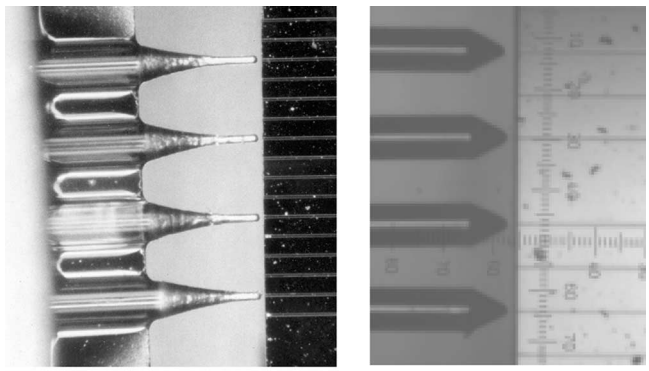

(a) (b)

Fig. 12. Fiber array. (a) Type E assembled with drawn fiber tips. (b) Type F assembled with mechanical polished fiber tips.

TABLE III
Measured Results of Two 4- and 8-Fiber Arrays Assembled With Different Fiber Tips as Shown in Fig. 12

| Array type | N [-] | Dx [μm] | Dy [μm] | Dz [μm] | η [dB] |
|---|---|---|---|---|---|
| E | 4 | 2.2 | 1.3 | 5 | -6 |
| E | 8 | 2.5 | 2.5 | 4 | -7.8 |
| F | 4 | 1.2 | 0.6 | 1 | -5.2 |
| F | 8 | 1.8 | 1.2 | 6 | -6.5 |

composed of four and eight fibers are characterized. First, the IR-spot distribution is measured, and after this, the coupling efficiency is determined. The fiber arrays are aligned to the same optical chip with waveguide loops that are used for the optical coupling experiments of the assembled fiber array in Section VI. The general conclusion is that the maximum IR-spot distribution of array type F is smaller than type E. The measured results are summarized in Table III; in the column are shown consecutively, the type of array, number of fibers $N$, the maximal focused IR-spot distribution between the fibers in lateral $x$-direction $D_x$, transversal $y$-direction $D_y$, longitudinal $z$-direction $D_z$, and the average coupling loss between the fibers and the waveguide $\eta$.

The coupling losses of both arrays assembled with four fibers are 6 dB and 5.2 dB for all fibers simultaneously for the fiber-array types E and F, respectively. Likewise, the averaged measured losses of arrays assembled with eight fibers are 7.8 dB and 6.5 dB for array types E and F, respectively. These losses are include 4.5 dB due to the relative large lens radii of the used fibers, which are 14–16 $\mu$m and the other remaining losses introduced by the inaccuracy of the focused IR spot. Compared with the results of the laser-welded-array assembly, the coupling efficiency is improved by a factor of 2.

## VIII. Conclusion

Laser-assisted adjustment is demonstrated for aligning fibers in an array over a range of 2–8 $\mu$m. Using this technology, four fibers are aligned with an accuracy of $\pm 0.25$ $\mu$m.

The smallest measured fine-tuning step is 0.05 $\mu$m. This step is limited because of the laser welder, which has limited adjustable parameters, namely the energy and welding time (3 or 5 ms). Other parameters such as weld-spot diameter, laser-pulse shape, and laser tail are fixed. However, these parameters can exert influence on the step size.

The coupling losses of the fiber array, assembled with commercially available lensed fibers are of the order of 2.9–3.5 dB. The fibers have radii of 5 $\mu$m and tapered wedge-shaped angles of 90 °. The physical waveguide dimensions are 0.6 $\mu$m x 3 $\mu$m. In contrast, the coupling losses of commercially available fiber arrays are of the order of 5.2–7.8 dB. These losses include the relative large lens radii of 14–16 $\mu$m and the inaccuracy of the focused IR spot.

## IX. Recommendation

The crosstalk in the "cross shaped" align frames can be reduced by a proper choice of physical sheet dimensions. The relation between shrinkage, material properties, and laser energy remains a subject of further research. Also, decreasing the fiber pitch from 0.5 mm to a standard pitch of 0.25 mm can be improved.

## References


[1] H. Yoshimura, "Future photonic networks and the role of InP-based devices," in *Proc. 2000 Int. Conf. Indium Phosphide Relat. Mater.,* May 14–18, pp. 3–6.

[2] M. K. Smit, "InP photonic integrated circuits," in *Proc. 15th Annu. Meet. IEEE/Lasers Electro-Opt. Soc.,* Nov. 10–14, 2000, vol. 2, pp. 843–844.

[3] S. Kaneko, M. Noda, K. Shibata, T. Aoyagi, H. Watanabe, T. Hatta, and K. Kasahara, "Novel fiber alignment method using a partially metal-coated fiber in a silicon V-groove," *IEEE Photon. Technol. Lett.*, vol. 12, no. 6, pp. 645–647, Jun. 2000.

[4] J. H. C. van Zantvoort, F. M. Huijskens, C. G. P. Herben, and H. de Waardt, "Fiber array pigtailing and packaging of an InP-based optical cross connect chip," *IEEE J. Sel. Topics Quantum Electron.*, vol. 5, no. 5, pp. 1255–1259, Sep.–Oct. 1999.

[5] R. H. Rediker, "Semiconductor diode luminescence and lasers—a perspective," *IEEE J. Sel. Topics Quantum Electron.*, vol. 6, no. 6, pp. 1355–1362, Nov.–Dec. 2000.

[6] L. G. Cohen and M. V. Schneider, "Microlenses for coupling junction lasers to optical fibers," *Appl. Opt.*, vol. 13, no. 1, pp. 89–94, Jan. 1974.

[7] R. Bachelot, C. Ecoffet, D. Deloeil, P. Royer, and D.-J. Lougnot, "Integration of micrometer-sized polymer elements at the end of optical fibers by free-radical photopolymerization," *Appl. Opt.*, vol. 40, no. 32, pp. 5860–5871, Nov. 2001.

[8] P. D. Bear, "Microlenses for coupling single-mode fibers to single mode thin waveguides," *Appl. Opt.*, vol. 19, no. 17, pp. 2906–2909, Sep. 1980.

[9] I. W. Marshall, "Low loss coupling between semiconductor lasers and single-mode fibre using tapered lensed fibres," *Br. Telecom Technol. J.*, vol. 4, no. 2, pp. 114–121, Apr. 1986.

[10] H. Kuwahara, M. Sasaki, and N. Tokoyo, "Efficient coupling from semiconductor lasers into single-mode fibers with tapered hemispherical ends," *Appl. Opt.*, vol. 19, no. 15, pp. 2578–2583, Aug. 1980.

[11] K. Shiraishi, H. Ohnuki, N. Hiraguri, K. Matsumura, I. Ohishi, H. Morichi, and H. Kazami, "A lensed-fiber coupling scheme utilizing a graded-index fiber and a hemispherically ended coreless fiber tip," *J. Lightw. Technol.*, vol. 15, no. 2, pp. 356–363, Feb. 1997.

[12] G. D. Khoe, J. Poulissen, and H. M. de Vrieze, "Efficient coupling of laser diodes to tapered monomode fibres with high-index end," *Electron. Lett.*, vol. 19, no. 6, pp. 205–207, 1983.

[13] J.-I. Yamada, Y. Murakami, J.-I. Sakai, and T. Kimura, "Characteristics of a hemispherical microlens for coupling between a semiconductor laser and single-mode fiber," *IEEE J. Sel. Topics Quantum Electron.*, vol. 16, no. 10, pp. 1067–1072, Nov. 1980.

[14] T. Alder, A. Stöhr, R. Heinzelmann, and D. Jäger, "High-efficiency fiber-to-chip coupling using low-loss tapered single-mode fiber," *IEEE Photon. Technol. Lett.*, vol. 12, no. 8, pp. 1016–1018, Aug. 2000.

[15] G. Eisenstein and D. Vitello, "Chemically etched conical microlenses for coupling single-mode lasers into single-mode fibers," *Appl. Opt.*, vol. 21, no. 19, pp. 3470–3474, Oct. 1982.

[16] H. M. Yang, S. Y. Huang, C. W. Lee, S. H. Wang, and W. H. Cheng, "High coupling tapered hyperbolic fiber microlens," in *Proc. 54th Electron. Compon. Technol. Conf.,* Jun. 1–4, 2004, vol. 2, pp. 1895–1898.

[17] H. M. Presby and C. R. Giles, "Asymmetric fiber microlenses for efficient coupling to elliptical laser beams," *IEEE Photon. Technol. Lett.*, vol. 5, no. 2, pp. 184–186, Feb. 1993.

[18] R. A. Modavis and T. W. Webb, "Anamorphic microlens for laser diode to single-mode fiber coupling," *IEEE Photon. Technol. Lett.*, vol. 7, no. 7, pp. 798–800, Jul. 1995.

[19] H. Sakaguchi, N. Seki, and S. Yamamoto, "High efficiency coupling from laser diodes into single mode fibers with quadrangular pyramid-shaped hemielliptical ends," in *3rd Int. Conf. Integr. Opt. Opt. Fiber Commun. Tech. Dig.*, Apr. 1981, pp. 78–79.

[20] E. Weidel, "Light coupling from a junction laser into a monomode fibre with a glass cylindrical lens on the fibre end," *Opt. Commun.*, vol. 12, no. 1, pp. 93–97, Sep. 1974.

[21] B. Sverdlov, B. Schmidt, S. Pawlik, B. Mayer, and C. Harder, "1 W 980 nm pump modules with very high efficiency," in *Proc. 28th Eur. Conf. Opt. Commun.,* Sep. 8–12, 2002, vol. 5, pp. 1–2.

[22] W. Hunziker, E. Bolz, and H. Melchior, "Elliptically lensed polarization maintaining fibres," *Electron. Lett.*, vol. 28, no. 17, pp. 1654–1656, 1992.

[23] A. Ogura, S. Kuchiki, K. Shiraishi, K. Ohta, and I. Oishi, "Efficient coupling between laser diodes with a highly elliptic field and single-mode fibers by means of GIO fibers," *IEEE Photon. Technol. Lett.*, vol. 13, no. 11, pp. 1191–1193, Nov. 2001.

[24] K. Shiraishi, H. Yoda, T. Endo, and I. Tomita, "A lensed GIO fiber with long working distance for the coupling between laser diodes with elliptical fields and single-mode fibers," *IEEE Photon. Technol. Lett.*, vol. 16, no. 4, pp. 1104–1106, Apr. 2004.

[25] M. K. Song, S. G. Kang, N. Hwang, H. T. Lee, S. S. Park, and K. E. Pyun, "Laser weldability analysis of high-speed optical transmission device packaging," *IEEE Trans. Compon. Packag., Manuf. Technol. B*, vol. 19, no. 4, pp. 758–763, Nov. 1996.

[26] G. M. Ghaoui, J. Lipson, R. S. Moyer, and T. S. Stakelon, "A method of achieving improved radial alignment in an optical package utilizing laser welding techniques," in *Proc. 39th Electron. Compon. Conf.,* May 22–24, 1989, pp. 372–373.

[27] S. C. Wang, H. L. Chang, C. Wang, C. M. Wang, and J. W. Liaw, "Post-weld-shift in semiconductor laser packaging," in *Proc. 49th Electron. Compon. Technol. Conf.,* Jun. 1–4, 1999, pp. 1159–1163.

[28] W.-H. Cheng, W.-H. Wang, and J.-C. Chen, "Defect formation mechanisms in laser welding techniques for semiconductor laser packaging," *IEEE Trans. Compon. Packag., Manuf. Technol. B*, vol. 19, no. 4, pp. 764–769, Nov. 1996.

[29] Y.-C. Hsu, Y.-L. He, M.-T. Sheen, Y.-C. Tsai, J.-H. Kuang, and W.-H. Cheng, "A novel fiber alignment shift measurement technique employing an ultra high precision laser displacement meter in laser-welded laser module packaging," in *Proc. 54th Electron. Compon. Technol. Conf.* Jun. 1–4, 2004, vol. 2, pp. 1903–1908.

[30] S.-G. Kang, M.-K. Song, S.-S. Park, S.-H. Lee, N. Hwang, H.-T. Lee, K.-R. Oh, G.-C. Joo, and D. Lee, "Fabrication of semiconductor optical

switch module using laser welding technique," *IEEE Trans. Adv. Packag.*, vol. 23, no. 4, pp. 672–680, Nov. 2000.
[31] J. H. C. van Zantvoort, G. D. Khoe, and H. de Waardt, "Fiber array-to-photonic-chip fixation and fine tuning using laser support adjustment," *IEEE J. Sel. Topics Quantum Electron.*, vol. 8, no. 6, pp. 1331–1340, Nov.–Dec. 2002.
[32] S. C. Wang, C. Wang, Y. K. Tu, C. J. Hwang, S. Chi, W. H. Wang, and W. H. Cheng, "Effect of Au coating on joint strength in laser welding for invar–invar packages," in *Proc. 46th Electron. Compon. Technol. Conf.,* May 28–31, 1996, pp. 942–945.
[33] R. Chanchani and P. M. Hall, "Temperature dependence of thermal expansion of ceramics and metals for electronic packages," *IEEE Trans. Compon. Hybrids Manuf. Technol.*, vol. 13, no. 4, pp. 743–750, Dec. 1990.
[34] Y. Nakamura, "The invar problem," *IEEE Trans. Magn.*, vol. 12, no. 4, pp. 278–291, Jul. 1976.
[35] A. A. Bernussi, L. Grave de Peralta, and H. Temkin, "High-precision characterization of single-mode optical fiber arrays," *J. Lightw. Technol.*, vol. 21, no. 6, pp. 1557–1561, Jun. 2003.
[36] K. Ozawa, S. Ogawa, H. Ishida, and Y. Hattori, "High-speed measuring equipment of fiber core position of optical fiber array using piezo actuator," in *Proc. IEEE Int. Conf. Robot. Autom.* May 21–27, 1995, vol. 1, pp. 672–678.
[37] E. Grard, J. L. Bris, M. Di Maggio, F. Dorgeuille, J.-Y. Emery, P. Bonno, and M. Renaud, "High performance packaging technique used for clamped gain semiconductor optical amplifier array modules fabrication," in *Proc. 48th IEEE Electron. Compon. Technol. Conf.,* May 25–28, 1998, pp. 1270–1273.

**Johan H. C. van Zantvoort** was born in Riethoven, The Netherlands, on November 21, 1968. He received the Graduate degree in applied physics from the Technical College of Eindhoven, Eindhoven, The Netherlands, in 1994.

He was with DAF Trucks Research, Philips Center for Manufacturing Technology, and Philips Novatronics Eindhoven, all in Eindhoven. Currently, he is with the Electro-Optical Communication Group, Eindhoven University of Technology, Eindhoven, where he is engaged in research on packaging technologies of integrated optical devices. He is the author or coauthor of more than 20 refereed papers and conference contributions. He has been associated with several European research programs such as ACTS BLISS, ACTS APEX, and IST METEOR. Currently, he is involved with the national research program IOP Precision Technology.

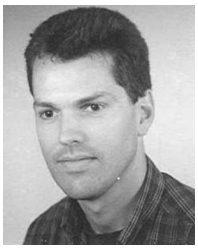

**Simon G. L. Plukker** was born in Eindhoven, The Netherlands, on July 2, 1968. He received the Graduate degrees in precision engineering from the Intermediate Technical School, Eindhoven, in 1989, and de Leidse Instrumentmakers School Nivo a+b, Delft, The Netherlands, in 1993.

From 1989 to 1991, he was with the Philips Natuurkundig Laboratorium, Eindhoven. Since 1991, he has been with the Gemeenschappelijke Technische Dienst, Eindhoven University of Technology, Eindhoven.

**Erwin C. A. Dekkers** was born in Veghel, The Netherlands, on April 21, 1968. He received the M.Sc. degree in mechanical engineering from Eindhoven University of Technology, Eindhoven, The Netherlands, in 1994.

From 1994 to 1999, he was a Mechanical Engineer at the Central Facility for Engineering and Manufacturing, Eindhoven University of Technology, where he designed and built numerous instruments and experimental setups for scientific research. From 1999 to 2003, he was the Chief, Mechanical Engineering, and thereafter a Project Manager within the same university. He is the author or coauthor of more than 15 papers published in international journals.

Mr. Dekkers is a member of the European Society of Precision Engineering and the Dutch Society of Precision Engineering. Since 1999, he has been a member of the Commission of Advice of the "Hoge School van Utrecht" for the Department of Mechanical Technology.

**Georgi D. Petkov** was born in Sofia, Bulgaria, on May 19, 1974. He received the M.Sc. degree in mechanical engineering from Sofia Technical University, Sofia, in 2001. Since 2003, he has been working toward the Ph.D. degree at Eindhoven University of Technology, Eindhoven, The Netherlands.

His current research interests include micro-optics.

**G. D. Khoe** (S'71–M'71–SM'85–F'91) was born in Magelang, Indonesia, on July 22, 1946. He received the Elektrotechnisch Ingenieur (*cum laude*) degree from Eindhoven University of Technology, Eindhoven, The Netherlands, in 1971.

Prior to 1973, he was with the Dutch Foundation's Fundamental Research on Matter (FOM) Laboratory on Plasma Physics, Rijnhuizen, The Netherlands. From 1973 to 1983, he was with Philips Research Laboratories, Eindhoven, where he was engaged in research on optical fiber communication systems. In 1983, he was a part-time Professor at Eindhoven University of Technology. In 1994, he became a Full Professor at this university and is at present the Chairman of the Department of Telecommunication Technology and Electromagnetics. He is currently engaged in research on single-mode fiber systems and components. He is the author or coauthor of more than 100 papers, invited papers published in international journals, and several book chapters. He is the holder of more than 40 U.S. patents. His current research interests include ultrafast all-optical signal processing, high-capacity transport systems, and systems in the environment of the users.

Prof. Khoe was General Co-Chair of the European Conference on Optical Communication 2001 and was a Founder of the IEEE Lasers and Electro-Optics Society (LEOS), Benelux Chapter. In 2003, he was appointed President of LEOS. He was the recipient of the MOC/GRIN award in 1997.

**Antonius M. J. Koonen** (M'00–SM'01) was born in Oss, The Netherlands, on October 20, 1954. He received the M.Sc. (*cum laude*) degree in electrical engineering from Eindhoven University of Technology, Eindhoven, The Netherlands, in 1979.

From 1979 to 1987, he was with Philips Telecommunicatie Industrie, Hilversum, The Netherlands. He was engaged in research on high-speed transmission systems and optical fiber systems for hybrid access networks. From 1987 to 2000, he was a Technical Manager in the Forward Looking Work Department, Bell Laboratories, Hilversum, within Lucent Technologies Network Systems Nederland, Hilversum. From 1991 to 2000, he was a part-time Professor at the University of Twente, Twente, The Netherlands, holding a Chair on Photonic Networks. In 1999, he was a Bell Labs Fellow, and in 2000, he was a part-time Professor at the Eindhoven University of Technology, Eindhoven. Since 2001, he has been a full-time Professor at this university, holding a Chair on Broadband Communication Networks in the Department of Telecommunication Technology and Electromagnetics. He is also managing the BraBant Breed-Band (B4) alliance, a joint precompetitive research cooperation on broadband network techniques and applications between the partners that include Lucent Technologies and Philips. He has participated extensively in several European cooperative research and development projects on wavelength-routed access networks. He is the author or coauthor of more than 65 papers on optical fiber communication published in international journals. He has been an auditor and reviewer of several national and European Commission projects. His current research interests include high-speed multiwavelength optical transmission and broadband access networks.

**Huug de Waardt** (A'06) was born in Voorburg, The Netherlands, in December 1953. He received the M.Sc. and the Ph.D. degrees in electrical engineering from Delft University of Technology, Delft, The Netherlands, in 1980 and 1995, respectively.

In 1981, he was with the Department of Physics, PTT Research, Leidschendam, The Netherlands, where he was engaged in research on performance issues of optoelectronic devices. In 1989, he was with the Transmission Department and was engaged in research on wavelength-division multiplexing high-bit-rate optical transmission. In 1995, he was an Associate Professor at Eindhoven University of Technology (TU/e), Eindhoven, The Netherlands, where he was engaged in research on high-capacity trunk transmission. He coordinated the participation of TU/e in ACTS Upgrade, ACTS BLISS, ACTS APEX, and IST FASHION. Currently, he is a Project Leader of the National Research Initiative Freeband Broadband Photonics (2004–2008). He is the author or coauthor of over 100 conference and journal papers published in international journals. His current research interests include high-capacity optical transmission and networking, integrated optics, and semiconductor optical amplifiers.

Dr. de Waardt is a member of the IEEE Lasers and Electro-Optics Society.